Resonant inelastic x-ray scattering on CO_2: Parity conservation in inversion-symmetric polyatomics

Johan Söderström,[1,*] Robert Stefanuik,[1] Franz Hennies,[2] Thorsten Schmitt,[3] Vladimir N. Strocov,[3] Joakim Andersson,[4] Brian Kennedy,[5] Justine Schlappa,[5,†] Alexander Föhlisch,[5,6] Annette Pietzsch,[5] and Jan-Erik Rubensson[1]

[1]*Department of Physics and Astronomy, Uppsala University, Box 516, SE-751 20 Uppsala, Sweden*
[2]*MAX IV Laboratory, Lund University, Box 118, SE-221 00 Lund, Sweden*
[3]*Swiss Light Source, Photon Science Division, Paul Scherrer Institut, CH-5232 Villigen PSI, Switzerland*
[4]*Solid State Electronics, Uppsala University, Box 534, SE-75121 Uppsala, Sweden*
[5]*Institute for Methods and Instrumentation in Synchrotron Radiation Research FG-ISRR, Helmholtz-Zentrum Berlin für Materialien und Energie, Albert-Einstein-Strasse 15, 12489 Berlin*
[6]*Institut für Physik und Astronomie, Universität Potsdam, Karl-Liebknecht-Strasse 24-25, 14476 Potsdam*

(Received 13 November 2019; accepted 17 April 2020; published 1 June 2020)

Resonant inelastic x-ray scattering (RIXS) spectra excited at the oxygen K edge of CO_2 are presented and discussed. Although excitation from a gerade initial state to the intermediate $1s^{-1}\pi^*$ state breaks the inversion symmetry due to strong vibronic coupling, RIXS excited at the corresponding resonance exclusively populates gerade vibrations in the gerade electronic ground state. This observation constitutes an experimental confirmation of the prediction that the parity selection rule applies in RIXS on an inversion-symmetric polyatomic system, provided that the total electronic-vibronic wave function is considered. Parity selectivity is used for assigning spectra to the population of electronically excited final states, a procedure hampered only when symmetry-breaking vibronic coupling in the *final* states is prominent. A RIXS spectrum excited in the Rydberg region is tentatively assigned using a simplified quasi-two-step model in which it is assumed that the electron in the Rydberg orbital excited in the first step remains as a spectator during the second decay step.

DOI: 10.1103/PhysRevA.101.062501

I. INTRODUCTION

The dipole approximation dictates that the parity of an inversion-symmetric system must change during a first-order radiative transition, and thus that the parity is unchanged in a second-order process like resonant inelastic x-ray scattering (RIXS), which involves two photons.

This process typically takes a system from an initial to a final state via an intermediate state with a core hole, and the notion that this core hole is localized at one atomic site is seemingly in conflict with inversion symmetry. Yet for homonuclear diatomic molecules it has been demonstrated that parity selectivity applies in the sub-keV range [1]. The conflict between preserved inversion symmetry and core-hole localization is only apparent, as symmetry-adapted ungerade and gerade states can be expressed in terms of a superposition of localized core-hole states [2]. In polyatomic inversion-symmetric molecules, on the other hand, electronic-vibronic coupling may lead to dynamic symmetry breaking and localization of the core hole.

In the x-ray emission spectrum of CO_2 it was demonstrated more than 30 years ago that oxygen core ionization is accompanied by excitations of antisymmetric stretch vibrations [3]. Thus, the inversion symmetry is broken as the two oxygen sites become inequivalent and the core hole localizes [4]. In RIXS spectra, vibronic coupling in the core excited state leads to the appearance of peaks that correspond to electronically dipole forbidden [5] transitions, i.e., peaks which must be assigned to a second-order scattering process, which change the parity of the electronic wave function. Insofar as the RIXS process is coherent, however, the total wave function, which includes both the electronic and vibronic degrees of freedom, the dipole approximation still predicts that parity is unchanged in the second-order process [6–8]. On the same footing as for homonuclear diatomics the "localized" core hole in the intermediate state can be described as a coherent superposition of inversion-symmetric states, with the difference that now the full electronic-vibronic wave function must be considered. In principle, this applies not only for small molecules like CO_2 but also for large inversion-symmetric systems like SF_6, C_6H_6, and C_{60}, and under substantial nuclear rearrangement including ultrafast dissociation. Inversion symmetry is central for current solid-state physics, especially in the context of topological materials [9]. Vibrational excitation in RIXS spectra of solids have been analyzed in terms of vibronic coupling, and dynamic symmetry breaking is considered to be crucial [10,11]. Note that in scattering to vibrational excitations of the gerade electronic ground state, breaking of the electronic-vibronic inversion symmetry presupposes decoherence. It can be anticipated that apparent decoherence may also be

*johan.soderstrom@physics.uu.se
†Current address: European X-Ray Free-Electron Laser Facility, Holzkoppel 4, 22869 Schenefeld, Germany.

observed for isolated systems, in cases where a large number of coupled vibrational modes and rotations are excited.

Recent technical advances make it possible to resolve individual vibrational excitations in RIXS not only of free molecules [12,13], liquids, and molecular systems in general [14], but also phonon excitations in materials with strong electron correlation [15,16], and further refinements are expected as new RIXS facilities come online at the diffraction limited synchrotron radiation sources [17].

Insofar as the RIXS process is coherent the initial and final states must have the same parity, and consequently, a parity change of the electronic wave function must be accompanied by a parity change of the vibrational wave function as well. With the technical advances this prediction can now be tested experimentally.

Here we present vibrationally resolved RIXS spectra excited at the oxygen K edge of CO_2. At the oxygen π^* resonance we demonstrate that the vibrational progression in scattering to the gerade electronic ground state exclusively show vibrational excitations of gerade symmetry. Thus the total symmetry of the wave function is preserved. Hence, our results are in full agreement with the coherent scattering picture, in spite of the substantial nuclear rearrangement in the intermediate state.

The RIXS spectra associated with electronically excited final states differ substantially from earlier predictions [18], a discrepancy which we attribute to the influence of bending mode vibrations due to the Renner-Teller effect, discussed in detail in Ref. [19], and extensive electronic-vibronic coupling in the *final* states [20]. In these cases symmetry assignment is difficult without advanced theory, and is beyond the scope of this paper.

In the second part of the paper we discuss Rydberg-excited states in terms of a simple two-step model [21], in which the population of Rydberg orbitals in a first excitation step is presumed to be preserved during the second emission step. We interpret possible deviations from this model as due to spectator electron shake processes during the decay step of the scattering process. We find no evidence for the violation of the parity selection rule when both electronic and vibronic wave functions are considered.

II. EXPERIMENT

The experiment was performed at the ADRESS beam line [22] of the Swiss Light Source, Paul Scherrer Institut, Villigen PSI, using the SAXES spectrometer [23]. The overall energy resolution was around 50 meV, allowing for separation of individual vibrations [12,13]. Linearly polarized incident radiation with the polarization vector parallel and perpendicular to the scattering plane was used, and the spectrometer measured scattered photons without polarization sensitivity perpendicular to the incident photon beam. Gas-phase measurements were facilitated using a flow-cell with a 100-nm-thick diamond-like window, separating the ultrahigh vacuum from the sample gas. Incoming and outgoing radiation passed through the same window, both at an angle of 45°.

The energy scale is calibrated using the Rydberg resonance in the x-ray absorption spectrum (XAS) near 540 eV [see Fig. 1(a)]. The main contributions to this peak are due to

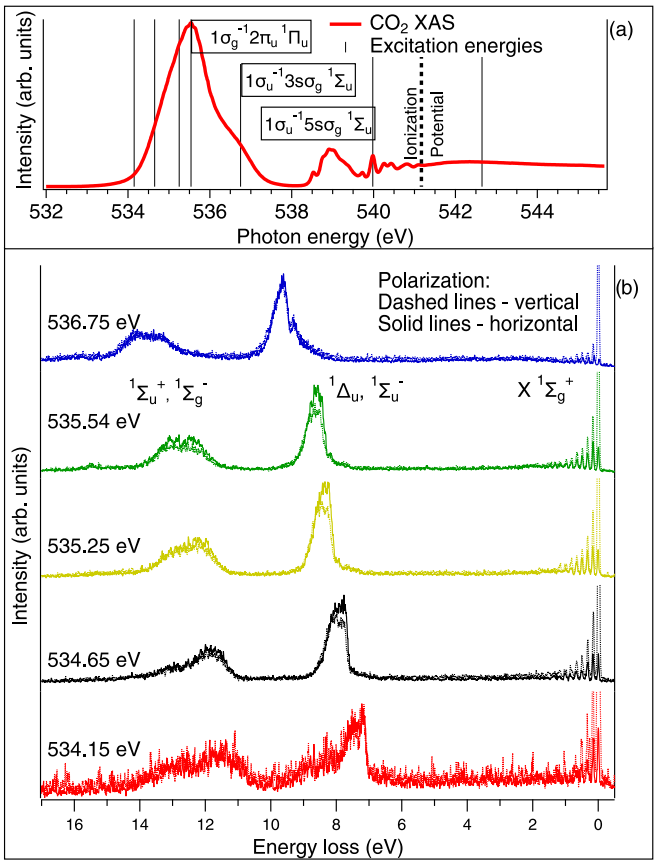

FIG. 1. (a) Absorption spectrum of CO_2 near the O1*s* edge. (b) RIXS spectra excited on the π^* resonance at energies marked by vertical lines in the absorption spectrum. See Fig. 3 for spectra measured at 539.98 and 542.65 eV. Note that the features around zero energy loss extend beyond the intensity scale (for vertical polarization) for all excitation energies. This increase in intensity for 0-eV energy loss is related to the elastic scattering of photons from the diamond-like window enclosing the gas cell and has no physical meaning for this experiment. See text for further details.

transitions to the vibrational ground state of the $1\sigma_u^{-1}5s\sigma_g$ and $1\sigma_g^{-1}4p\pi_u$ states [24,25]. We used 539.97 eV for the $1\sigma_u^{-1}5s\sigma_g$ resonance given in Ref. [26]. As several other transitions contribute to intensity in this energy region the peak appears to be shifted to slightly higher photon energy by approximately 10 meV.

III. RESULTS AND DISCUSSION

A. Overview

The ground state of the carbon dioxide molecule is $1\sigma_g^2 1\sigma_u^2 \ldots 4\sigma_g^2 3\sigma_u^2 1\pi_u^4 1\pi_g^4\ ^1\Sigma_g^+$. In the symmetric representation the main resonance in the XAS spectrum [see Fig. 1(a)] at 535.5 eV is assigned to transitions to the $1\sigma_g^{-1}2\pi_u\ ^1\Pi_u$ state, and the high-energy shoulder around 536 eV to the $1\sigma_u^{-1}3s\sigma_g\ ^1\Sigma_u$ Rydberg state [26,27], which also has valence orbital contributions [19]. Around 539 eV there is a complex feature due to several contributing transitions, and the sharp peak just below 540 eV, that we use for calibration, is dominated by transitions to the vibrational ground state

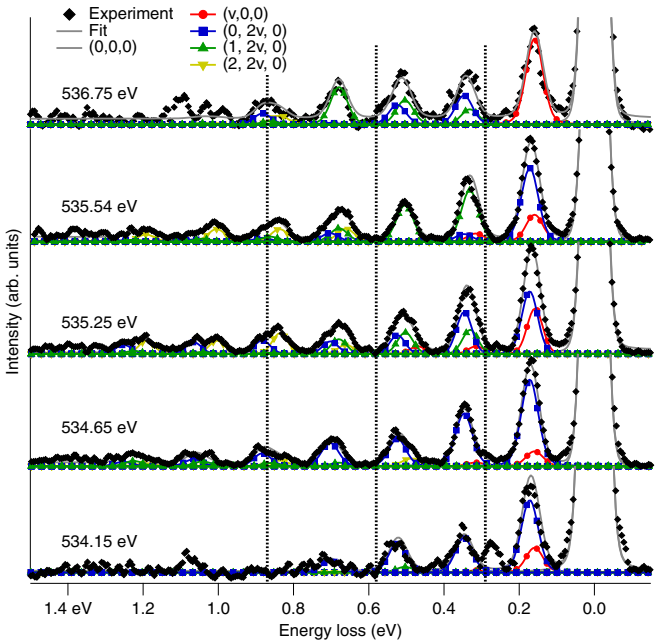

FIG. 2. The vibrational excitations fitted with vibrational modes of gerade symmetry: even number of quanta of the bending mode $2n\nu_2$ (blue, at slightly higher energies than) the symmetric stretch mode ν_1 (red), and combinations thereof (green and yellow, at values between red and blue). No peaks are observed at the energy positions of the antisymmetric stretch vibrations ν_3, indicated by dashed vertical bars in the figure, or of odd number of bend modes $(2n+1)\nu_2$.

of the $1\sigma_u^{-1}5s\sigma_g$ Rydberg state [26]. The vertical bars in Fig. 1(a) indicate the photon energies where the RIXS spectra discussed in this paper are excited.

For energy losses up to 2 to 3 eV the RIXS spectra in Figs. 1 and 2 show resolved vibrational progressions in transitions back to the $X\ ^1\Sigma_g^+$ electronic ground state. The feature around 8-eV energy loss has been assigned to electronically dipole-forbidden $1\pi_g^{-1}2\pi_u\ ^1\Delta_u, ^1\Sigma_u^-$ states [5,18]. Around 12 to 14 eV there is a double peak which can be assigned to the $1\pi_u^{-1}2\pi_u\ ^1\Sigma_g^-$ and dipole-forbidden $1\pi_g^{-1}2\pi_u\ ^1\Sigma_u^+$ final states [18]. The spectra show a strong excitation-energy dependence.

It is well established that scattering to electronically dipole-forbidden ungerade final states directly demonstrates dynamic symmetry breaking in the intermediate state [5,6,18]. Analysis has shown that a Jahn-Teller-type coupling via the antisymmetric stretch mode mixes the intermediate $1\sigma_g^{-1}2\pi_u\ ^1\Pi_u$ and the near-degenerate dipole-forbidden $1\sigma_u^{-1}2\pi_u\ ^1\Pi_g$ states to form symmetry-broken electronic wave functions Ψ_L and Ψ_R with core holes localized on the left and right oxygen atoms [6,8], respectively, $\Psi_L = \frac{1}{\sqrt{2}}(^1\Pi_g + {}^1\Pi_u)$ and $\Psi_R = \frac{1}{\sqrt{2}}(^1\Pi_g - {}^1\Pi_u)$. Thereby the scattering channels to electronically dipole-forbidden final states are opened. A Kramers-Heisenberg treatment of the RIXS process including both the electronic and vibronic parts, predicts that parity selectivity is preserved for the total wave function [6–8]. The detuning from the main resonance is not sufficiently large for restoration of the electronic inversion symmetry at large detuning, which was demonstrated in Ref. [5].

If the *final* state can be described within the Born-Oppenheimer approximation the symmetry of the electronic and vibronic states can be addressed separately, and as the total wave function in the present case should be gerade, the parity of the final electronic state must be the same as the parity of the vibrational state in order for the total wave function to be gerade. The observation of any ungerade vibrational excitations in an electronically gerade final state would imply a violation of the Kramers-Heisenberg approach and suggest that the extensive nuclear rearrangement in the intermediate state leads to decoherence, in the sense that the description of the intermediate states as coherent linear combinations of gerade and ungerade states would no longer be valid.

B. Vibrational excitations in the electronic ground state

The vibrational excitations associated with transitions to the $X\ ^1\Sigma_g^+$ gerade electronic ground state are especially well suited to address the electronic-vibronic parity selection rules, as the coherent description strictly requires the vibrational excitations to be gerade.

The vibrational progression show seven to eight well-resolved peaks (see Fig. 2). The spacing between the peaks is around 0.16 eV, and whereas the lowest-energy-loss peaks are fairly sharp, the peaks at higher-energy loss have internal structure and gradually develop to a double feature. The vibrational excitations in the CO_2 ground state have been analyzed in detail [28], and it was found that the fundamental energies of the ungerade vibrations are 0.29 eV for the antisymmetric stretch (ν_3) and 0.083 eV for the bend (ν_2) modes.

We mark 0.29 eV energy-loss (ν_3) intervals in Fig. 2 by dashed vertical lines, and it is obvious that excitation corresponding to such energy losses are absent. The peak at 0.87 eV obviously is a part of a different progression. Easily observable intensity corresponding to a multiple of 0.083-eV (ν_2) excitations is also lacking.

Although the bend modes have ungerade (Π_u) symmetry, excitation of an *even* number of quanta has gerade symmetry. It has been recognized that the excitation of an even number of quanta of the bend mode may have the same (Σ_g^+) symmetry and almost the same energy as one quantum of the symmetric stretch mode (ν_1). This gives rise to a Fermi resonance; substantial wave-function mixing which perturbs the energy positions and changes the intensities, thereby complicating the analysis of the vibrations. In Fig. 2 we use the energy positions of the experimental features assigned in Ref. [28] in fitting the RIXS features. The fit in terms of vibrations with gerade symmetry is excellent, implying that symmetric vibrations are the totally dominant vibrational excitations in the final electronic state. This observation supports the validity of the electronic-vibronic parity selection rules, and the coherent description of the scattering process.

In view of the violent nuclear dynamics in the intermediate state, with a multitude of antisymmetric stretch- and bend-mode excitations, this is a result which may seem surprising. It is well known that the Renner-Teller effect lifts the degeneracy of the $1\sigma_g^{-1}2\pi_u\ ^1\Pi_u$ and $1\sigma_u^{-1}2\pi_u\ ^1\Pi_u$ states so that electronically dipole-forbidden states are observed in RIXS [5]. This vibronic coupling leads to highly bent molecules, and experiments suggest very small bond angles

in the intermediate state [29]. In a simple picture, appreciable bend-mode vibrations are therefore expected. This is in line with the fitting results, according to which the progressions are dominated by even bend-mode ($2n\nu_2$) vibrations (see Fig. 2). The fitting results also show that the broadening and fine structure within each peak, especially obvious for energy losses higher than 0.6 eV, can be interpreted in terms of a combination of symmetric stretch and an even number of bend excitations. This picture is complicated by the Fermi resonance, and we note that the small energy spacing between the vibrational states makes a definite assignment based on the fit uncertain. It is, however, obvious that the pure symmetric stretch vibration dominates only for the first excitation at 536.75 eV. At this excitation energy the intermediate state is $1\sigma_u^{-1}3s\sigma_g\,{}^1\Sigma_u$, and the Rydberg character suggests that much less bending is initiated, compared to the $1\sigma_g^{-1}2\pi_u\,{}^1\Pi_u$, inline with the observed results.

There is a noticeable excitation-energy dependence of the vibrational excitations. Clearly the vibrational progression is shortened for excitation at 534.15 eV, corresponding to a detuning of $\Omega \approx 1.4$ eV below the peak at 535.54 eV. Using the scattering duration concept [30], and assuming a core-hole lifetime width of $\Gamma \approx 0.165$ eV [31,32], it can be estimated that the scattering duration changes from $\tau \approx 4$ fs on resonance to $\tau = \frac{\hbar}{\sqrt{\Omega^2+\Gamma^2}} \approx 0.5$ fs. This is qualitatively inline with the reduced vibrational progression upon detuning.

Finally, we emphasize that within the experimental accuracy there is no evidence for intensity corresponding to a symmetry-breaking odd bend mode [$(2n+1)\nu_2$] or antisymmetric ν_3 vibrations. Thus we find no evidence for violation of the parity selection rules, at the very resonance, which has earlier been used as a showcase for dynamic symmetry breaking [5,6,18]. The coherent description of the scattering process can be applied to the π^* resonance in CO_2, if the total wave function is considered.

This result is significant when RIXS is applied to larger symmetric molecules, molecular solids, and condensed matter with symmetry-dependent properties. In contrast to what is reported here, vibrational excitations in solids have earlier been assigned to dynamic symmetry breaking [10,11], implying a loss of coherence during the scattering process. It is anticipated that such phenomena can be investigated in detail as vibronic excitations in solids are resolved at the new generation high-resolution RIXS facilities.

C. Electronic-vibronic excitations

The energy loss in the 7–9 eV range [see Fig. 1(b)] is assigned to the lowest electronically excited ${}^1\Delta_u$ and ${}^1\Sigma_u^-$ states with $1\pi_g^{-1}2\pi_u$ as the leading configuration, and in addition there is an allowed ${}^1\Pi_g$ state of $1\pi_g^{-1}3s\sigma_g$ Rydberg character in the same energy region [20]. The latter is expected to gain intensity around 536.75 eV, corresponding to the $1\pi_g^{-1}3s\sigma_g$ excitation, as the intermediate $1\sigma_u^{-1}3s\sigma_g\,{}^1\Sigma_u$ state is contributing to the high-energy flank of the main absorption feature. It has been shown that the Born-Oppenheimer approximation cannot be applied to the description of these states [20], and therefore the symmetry of the vibrations cannot be separately addressed. The Renner-Teller effect breaks the symmetry and mixes these *final* states, most of them are predissociative, and the states are subject to avoided crossings and conical intersections [20,33] suggesting that it may be misleading to use the inversion symmetric notation for these final states [19]. Yet, for very large detuning, where the short scattering duration seems to inhibit vibronic coupling in the intermediate state, the peak corresponding to these final states does loose intensity [5]. This is to be expected if the electronic final states to some extent retain ungerade symmetry, which is forbidden in RIXS.

The analysis of the polarization dependence (Fig. 1) is hampered since the observed features are associated with several final states, as indicated in Fig. 1. For the linear molecule it is expected that the ratio between the intensity excited with vertical (I_v) and horizontal (I_h) polarization is

$$\frac{I_v}{I_h} = \frac{2+R_\Lambda}{2-2R_\Lambda}, \tag{1}$$

where $R_{\Sigma^+} = 0.4$, $R_\Delta = 0.1$, and $R_{\Sigma^-} = -0.5$ [6], which implies that $\frac{I_v}{I_h} = 2$ for $\Sigma_{g,u}^+$ final states, $\frac{I_v}{I_h} = \frac{7}{6}$ for the $\Delta_{g,u}$ final states, and $\frac{I_v}{I_h} = \frac{1}{2}$ for the $\Sigma_{g,u}^-$ final states.

We now turn our attention to the experimentally observed ratios. The peak at 8–9 eV, assigned to Δ_u and Σ_u^- final states, shows $\frac{I_v}{I_h} \approx 0.9$ [Figs. 1(b) and 1(c)]. Assuming equal contribution from both final states, an average theoretical value for the linear molecule is $\frac{I_v}{I_h} = \frac{\frac{7}{6}+\frac{1}{2}}{2} = \frac{5}{6}$ which is close to the experimental observation.

The peak at 12–14 eV, assigned to Σ_u^+ and Σ_g^- states also gives $\frac{I_v}{I_h} \approx 0.9$. Again, assuming an equal contribution from the two final states, an average theoretical value for the linear molecule is $\frac{I_v}{I_h} = \frac{2+\frac{1}{2}}{2} = \frac{5}{4}$ which slightly deviates from the experimental observation.

For losses larger than 6 eV, the energy-loss features in the RIXS spectra shift towards higher losses when the excitation energy increases across the π^* resonance [see Fig. 1(b)], i.e., the features stay at constant energy on an emission energy scale. Such apparent independence of the excitation energy is often taken as an indication that specific excitations in the first step do not influence the second emission step. In this case this instead indicates that excess vibrational energy absorbed in the intermediate state is directly transferred to a quasicontinuum of electronic-vibronic final states in this energy region. Thus, while the shape of the peaks are similar in the 534.65–535.54 eV excitation-energy range, final states at the higher excitation energies comprises substantially higher vibrational excitations. A similar behavior is observed for small molecules in cases where the potential surfaces of the intermediate and final states are alike: higher vibrational excitations in the intermediate state give higher excitations in the final state, resulting in emission at almost constant emission energy [34]. The one-step nature of the RIXS process, demonstrated in the analysis of the vibrationally resolved part of the spectrum, shows that the decoherence, that excitation-energy independence seems to indicate, is only apparent, and that the process is in fact fully coherent.

Note also that at the lowest excitation energy, the spectral shape is significantly different, apparent around 8–9-eV energy loss, with a sharp edge around 7.1-eV energy loss. The later energy is lower than any feature in the VUV absorption spectrum, and lower than the O ^1D + CO(X)

photodissociation threshold at 7.41 eV [28]. For bent molecules nondissociative states are indeed predicted below this threshold [20,28,35], and the data suggest that low-energy vibrations in such an electronic state is reached via the intermediate state dynamics, which also includes Renner-Teller coupling.

The overall shape of the RIXS spectra excited across the π^* resonance is in line with the earlier RIXS theory [18], where, e.g., the predicted double structure in the peak at 12–14-eV energy loss is clearly observed. The relative intensity decrease of the high energy-loss partner of the peak upon detuning the excitation energy corroborates its assignment to an electronically dipole forbidden final state, whereas the low energy-loss partner is assigned to transitions to an allowed final state. In Ref. [18] RIXS spectra were predicted to comprise extensive well-resolved vibrational progressions with an assumed experimental resolving power much lower than for the spectra presented here. We believe that the discrepancy is due to interactions neglected in the theory, e.g., the omission of bend-mode excitations, and state mixing in the final states. The present results suggest that both these effects are essential to understand the RIXS spectra.

Finally, we note that the spectrum excited at 536.75 eV differs substantially from spectra excited at lower energies. This is due to the contribution of a $1\sigma_u^{-1}3s\sigma_g\ ^1\Sigma_u$ Rydberg state to the resonance, with an expected population of final states with a valence hole and the excited $3s\sigma_g$ electron as a spectator. The sharp peak at 9.3-eV energy loss (see Fig. 1) corresponds to a feature found in electron-energy loss spectra [36], which indeed was assigned to the $1\pi_g^{-1}3s\sigma_g\ ^1\Pi_g$ state, with likely valence mixing.

D. Excitations above the ionization limits

To analyze the spectrum excited on the Rydberg resonance at 539.98 eV, we compare to the spectrum excited at 542.65 eV, above the ionization thresholds (Fig. 3). The comparison on the emission energy scale is relevant if we assume a quasi-two-step picture of the RIXS process where the electron excited in the first excitation step is regarded as a spectator during the second decay step. The Rydberg-excited spectrum will be further discussed in a model based on this simple picture below. The intermediate state at above-threshold excitation has the spectator electron in the continuum, where the only influence on the emission is that its energy distribution is reflected in the broadening of the spectral features due to the finite lifetime of the intermediate state [37]. The similarity of the two spectra (Fig. 3) shows that this comparison is a good starting point for the analysis. As usual the spectra can be put on the final-state energy scale by subtracting the emission energy from the excitation energy. For above-threshold excitation we use the core-level ionization energy, 541.17 eV [24,27,32] as reference.

In the spectrum excited above the ionization limits emission from all symmetries is allowed and we expect transitions to the outermost $1\pi_g^{-1}\ ^2\Pi_g$, $1\pi_u^{-1}\ ^2\Pi_u$, $3\sigma_u^{-1}\ ^2\Sigma_u$, and $4\sigma_g^{-1}\ ^2\Sigma_g$ ionic final states, with the adiabatic transitions at 527.39, 523.86, 523.10, and 521.78 eV, respectively [38,39]. This enables the assignment of the main features

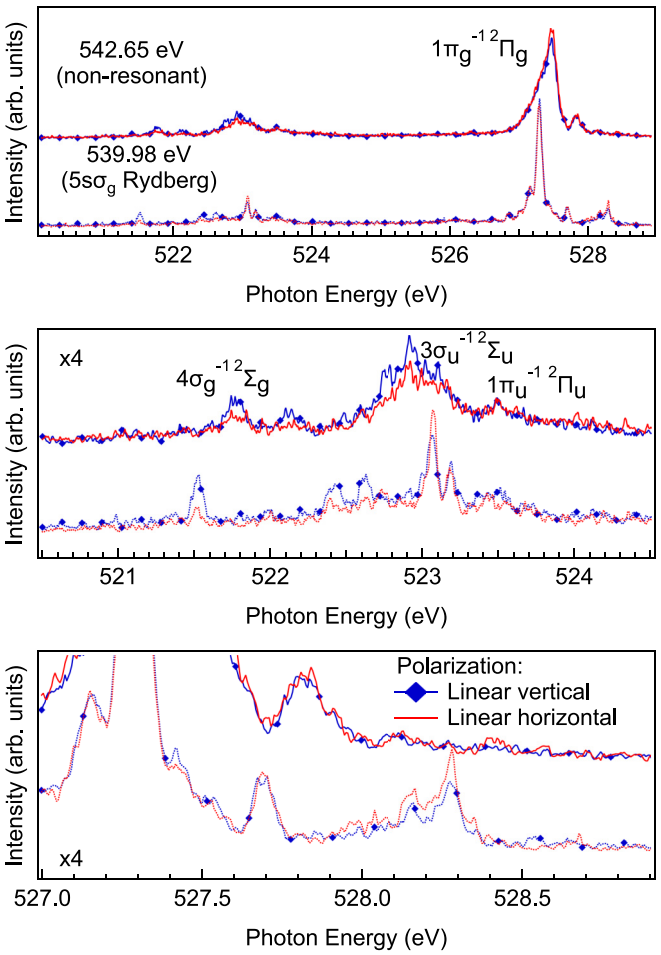

FIG. 3. RIXS spectra recorded for both linear horizontal (LH) and linear vertical (LV) polarization, excited above threshold and at the Rydberg resonance at 539.98 eV. Above threshold transitions to the $1\pi_g^{-1}\ ^2\Pi_g$ (527.39 eV), $1\pi_u^{-1}\ ^2\Pi_u$ (523.86 eV), $3\sigma_u^{-1}\ ^2\Sigma_u$ (523.10 eV), and $4\sigma_g^{-1}\ ^2\Sigma_g$ (521.78 eV) ionic final states are seen (see Refs. [38,39]). We used the $4\sigma_g^{-1}\ ^2\Sigma_g$ final state to set the energy scale. These well-known features are then used to assign the main features in Fig. 3. As expected there are some intensity differences between the final states observed in LH compared to LV which are briefly discussed in the text, and the lifetime broadening is clearly visible in the nonresonant spectrum. The two bottom spectra show a zoom-in of the low-intensity regions highlighting the differences between the polarization states in these energy regions.

in the spectrum excited above the ionization threshold (see Fig. 3), in agreement with earlier studies [3,5,40].

Fine structure in the emission bands can be attributed to vibrational excitations, and it was shown early on that excitations of the core-hole localizing antisymmetric stretch mode in the intermediate state must be taken into account [3,41]. Thus, for excitation above the ionization threshold, we expect emission not only from the vibronic ground state, but also appreciable emission from the first antisymmetric stretch excitation in the core ionized state ($\nu_3' = 1$) at 307-meV [31] higher emission energy. Emission from these states to $\nu_3'' = 1$ final states is expected to largely overlap with transitions between the vibronic ground states $\nu_3' = 0 \rightarrow \nu_3'' = 0$, whereas transitions from $\nu_3' = 1$ to $\nu_3'' = 0$ final states should

be shifted towards higher energies on the order 307 meV. We note that several features, e.g., $4\sigma_g^{-1}$ and $1\pi_g^{-1}$ peaks have replicas on the high-energy side, see Fig. 3. We assign these to such "vibronic-gain" transitions, and we note that the observation of such antisymmetric stretch excitations in the x-ray emission spectrum was the first observational evidence of ultrafast symmetry breaking in molecular core ionization [3]. The present data confirm the predictions in the early paper in detail, especially for the $1\pi_g^{-1}$ final state.

We note a slight polarization dependence, where emission from orbitals of π symmetry is enhanced relative to emission from σ orbitals when the polarization of the incident radiation changes from horizontal to vertical. This implies that the continuum just above threshold is dominated by σ symmetry, confirming results from symmetry-resolved absorption measurements [26].

For diatomics RIXS sensitivity to the parity of the continuum is well established [1], here such an analysis must await theoretical development.

E. Rydberg excitations

Compared to the spectrum excited above threshold the overall shape of the spectrum is retained when exciting on the Rydberg resonance at 539.98 eV (see Fig. 3), inline with the assumption that there is one dominating intermediate state, where the Rydberg electron couples only a little to the rest of the system, and primarily acts as a spectator during the radiative decay. At 539.98 eV the absorption spectrum is dominated by the sharp $1\sigma_u^{-1}5s\sigma_g\ ^1\Sigma_u$ Rydberg resonance, and consequently the most intense peak around 527.3 eV in the RIXS spectrum is dominated by scattering to the electronically allowed $1\pi_g^{-1}5s\sigma_g\ ^1\Pi_g$ final state.

Also at lower emission energy, in the 521–524-eV region, we observe features which are narrower than the lifetime width of the intermediates state. These features are assigned to transitions to final states far above the $1\pi_g\ ^2\Pi_g$ ionization limit at 13.78 eV [39], corresponding to emission energies below 526.2 eV. Most of these states are difficult to observe in VUV absorption, electron-energy loss, and other low-energy methods [36,42,43] due to the high background of continuum states. We assign the single sharp peak at 521.5 eV, corresponding to transitions to a final state with an energy of 18.48 eV, to the ground vibrational state of the $4\sigma_g^{-1}5s\sigma_g\ ^1\Sigma_g^+$ state, i.e., a state where the hole is in an orbital of primarily C $2s$ character and the electron in a gerade Rydberg orbital.

The polarization dependence for $^1\Sigma_g^+$ for the linear molecule is given by $\frac{I_v}{I_h} = 2$, which is fully confirmed by the observation of the enhancement of the signal at vertical polarization [see Fig. 1(b)]. The polarization dependence of transitions to final states at 522.4 and 522.6 eV (see Fig. 3), corresponding to final-state energies 17.58 and 17.38 eV, also implies $^1\Sigma^+$ symmetry.

By comparing to the spectra excited above threshold it is natural to assign these peaks to electronically dipole-forbidden transitions to the $3\sigma_u^{-1}5s\sigma_g\ ^1\Sigma_u^+$ final state. If this state indeed is inversion symmetric, the scattering channel would only be allowed by antisymmetric vibrational excitations, and we tentatively assign the peaks to such excitations in $3\sigma_u^{-1}5s\sigma_g\ ^1\Sigma_u^+$. Using the polarization dependence the double peak at 523.1 eV, corresponding to 16.88-eV final-state energy, can be assigned to the $1\pi_u^{-1}5s\sigma_g\ ^1\Pi_u$ final state. Again, for the total final-state wave function to be symmetric the vibrational excitations must be antisymmetric. As in the case of valence excitations, vibronic coupling in the final states may hamper the assignment in terms of separate vibronic and electronic excitations.

In the following we turn our attention to the spectral region around the main peak around 527.3-eV emission energy, which primarily is assigned to the $1\pi_g^{-1}5s\sigma_g\ ^1\Pi_g$ final state (see Fig. 3), and show it on the energy-loss scale in Figs. 4(b) and 4(c).

Additional features that appear close to the main peak [see Fig. 4(b)] cannot be exclusively explained by vibrational excitations in the same electronic final state, indicating that also other electronic states are populated. In a two-step picture the population of final states in which the Rydberg electron is in an orbital which is not excited at resonance can be thought of as spectator shake-up or shake-down during the second emission step of the process. Such processes have earlier been termed radiative Auger [44] and radiative electron rearrangement [45]. However, the cross section for such processes is small. For atoms it has been predicted that the probability for Rydberg-spectator shake processes is small [46], and for the N_2 molecule we showed that present state-of-the-art close-to-threshold excited Rydberg RIXS spectra can be described without taking such processes into account [21]. For the analysis of the N_2 spectrum we developed a simple model to account for apparent Rydberg shake process in the decay step [21]. The model showed that the observations could be understood by taking Lorentzian-tail excitations into account, i.e., by assuming that the probability for excitation of a certain final state is determined by the finite Lorentz amplitude of the state at each specific excitation energy. Here we apply the same model to the $1\sigma_u^{-1}5s\sigma_g\ ^1\Sigma_u$ resonance in CO_2.

To perform the analysis a series of assumptions has to be made, and we describe the procedure below. We model the absorption spectrum to estimate the tail contributions for close-lying states [see Fig. 4(a)]. We use the assignments of Ref. [26] and to optimize the model we recalculate the quantum defects (QD) with the ionization threshold 541.17 eV from Refs. [24,27,32]. To fit the data properly the QD for the first vibrational component of the $s\sigma_g$ series (labeled $s\sigma_g$ + 001 in Fig. 4) was changed from 1.63 to 1.66 for $n = 5$. In addition to this we note that the tabulated QD for $7\sigma_g$ deviates strongly from others in the same series, we thus chose to keep the same QD for $7\sigma_g$ as for $6\sigma_g$.

Here we also make the model assumption that the vibrational excitations in the core excited Rydberg states are the same as in core-level photoemission [31], and we simulate the broad valence-mixed $4s\sigma_g$ resonance around 539 eV by multiple *ad hoc* Lorentzians. For all states we use a lifetime broadening of 165 meV [31,32].

The simple model assumes that a Rydberg orbital is populated in a first excitation step and stays in this orbital during the second decay step of the scattering process, and that the quantum defect is identical in the intermediate and final states. As seen in Figs. 4(b) and 4(c) the model gives intensity for not only the main peak which is dominated by the $1\pi_g^{-1}5s\sigma_g$ (12.78 eV) final state, but it also gives appreciable

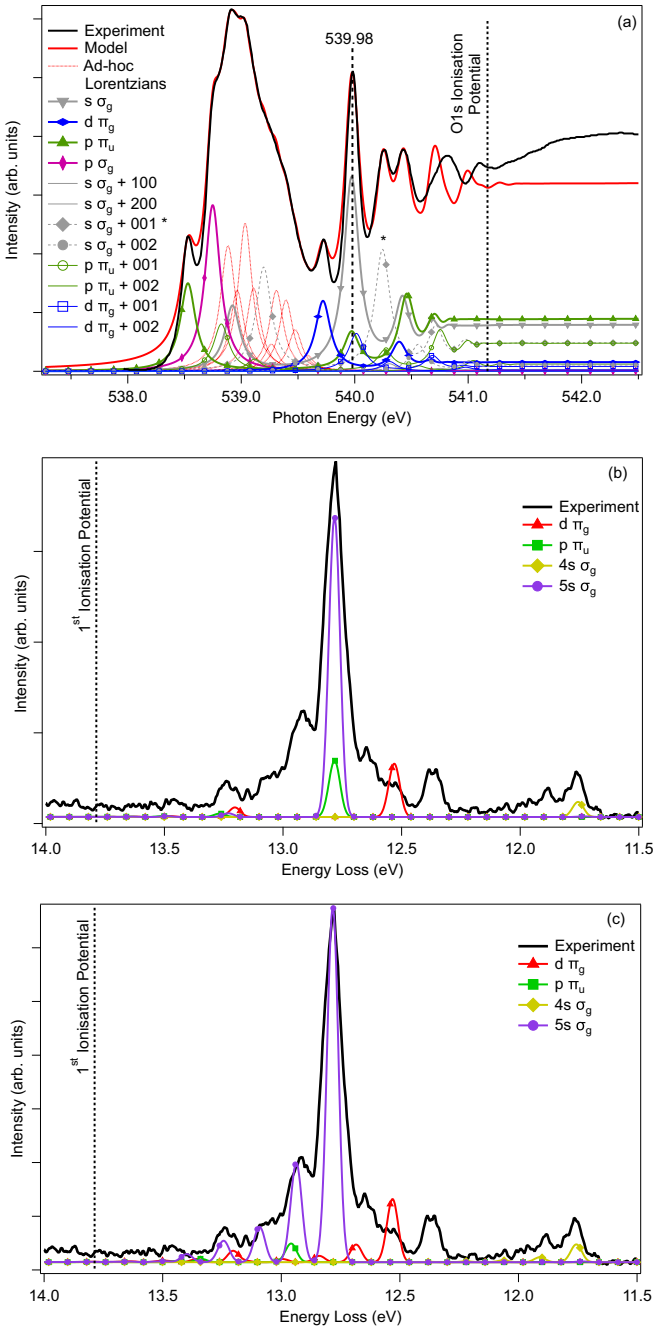

FIG. 4. (a) The absorption spectrum close to the O1s ionization threshold, and the model used to estimate the tail excitations when the excitation energy is tuned to 539.98 eV. The * of $s\sigma_g + 001$ indicates that the QD for $n = 5$ in this series deviates from tabulated values, this was needed to get a reasonable fit around 540 eV. (b) The contributions to the final states without vibrational excitations in a zoom-in of the Rydberg-excited RIXS spectrum, which is also shown in Fig. 3. The model assumes that energy spacing between the Rydberg states is the same as for the core-excited Rydberg states assigned in Refs. [26,27]. (c) Estimated dipole-allowed stretch vibrations are added to fit the main peak, and the intensity ratios are assumed to be the same for the other gerade states.

spectral weight for final state $1\pi_g^{-1}4s\sigma_g$ (11.75 eV), $1\pi_g^{-1}3d\pi_g$ (12.55 eV), and $1\pi_g^{-1}4p\pi_u$ coinciding with the main peak. Around 13.3-eV intensity for the $1\pi_g^{-1}6s\sigma_g$, $1\pi_g^{-1}4d\pi_g$, and $1\pi_g^{-1}5p\pi_u$ are predicted by the model. In spite of the simplifications this model gives a tentative assignment and a qualitative understanding of the main features. To account for the remaining discrepancies we discuss vibrational excitations in the next step [see Fig. 4(c)]. Again, we assume that the Rydberg electron has little influence on the potential surface, so that the vibrational energies for the ionic ground state [39] can be used. Further, we assume that only the symmetric stretch is excited in electronically gerade states, and only the antisymmetric stretch in electronically ungerade states.

With the inclusion of vibrational excitation this simple model captures most features of the spectrum [see Fig. 4(c)]. This concordance suggests that the spectrum can be understood without consideration of Rydberg shake processes, and that it does not provide evidence for any violation of dipole selectivity.

In the following we briefly discuss the remaining discrepancies. The features are broader than what is accounted for by the instrumental resolution and the model assumptions. We believe that this is due to the omission of bending-mode vibrations, which remain unresolved.

The intensity of the $1\pi_g^{-1}4s\sigma_g$ state is not fully accounted for in the model, nor is the vibrational energy spacing. We believe that, due to valence-Rydberg mixing, its potential surface is different from that of the ionic surface. The peak at 12.4 eV is tentatively assigned to the $1\pi_g^{-1}3d\pi_g$ states, thus requiring a low-energy shift of around 0.15 eV of the predicted peak position. This would indicate that the $3d\pi_g$ electron is more tightly bound to the final-state valence hole than to the intermediate-state core hole, in line with the assignment of the corresponding electron energy loss [42], and VUV optical [43] feature at 12.27 eV. With the same techniques a feature at 12.50 eV is assigned to $1\pi_g^{-1}4p\pi_u$ final states, and we speculate that also this electronically dipole-forbidden state is pulled down below the main peak and may contribute to the intensity in this region.

To describe the spectrum in detail, theoretical development is called for, and if shake processes are found to be significant they must take into account not only lifetime-vibrational but also lifetime-electronic-state interference.

IV. CONCLUSION

The complex RIXS spectra excited at the oxygen K edge of CO_2 allows for a number of conclusions. The coherent description of the RIXS process is manifested by the observation that only gerade vibrational modes are excited in scattering to the electronic ground state. This implies that parity is conserved in the RIXS process as dictated by the dipole selection rule, also when extensive bend and antisymmetric stretch vibrations are excited in the intermediate state. Electronically excited final states are accompanied by substantial vibronic excitations. They are typically not described within the Born-Oppenheimer approximation, which hampers symmetry identification. Bend-mode excitations, omitted in earlier theoretical treatments, turn out to be crucial for the description of the spectra. Spectra excited above the ionization limit clearly resolve emission from antisymmetric stretch vibrations in the ion, thereby confirming early predictions

from the pioneering work on dynamic symmetry breaking. The polarization dependence confirms that the continuum just above threshold predominantly has σ character. Finally, a Rydberg resonance selectively populates final states, high above the valence ionization limit. These states, which cannot be identified by low-energy methods, are assigned via the polarization dependence of the spectra. Apparent radiative electron rearrangement, or Rydberg electron shake processes, in the decay step is explained using a simple two-step model that assumes that the Rydberg electron excited in the first step stays as a spectator during the decay, takes the Lorentzian tails of all contributing intermediate states into account, and requires that parity is conserved. This model accounts for the gross features of the spectrum.

In general the observations reported here demand theoretical development. This is especially urgent as larger inversion symmetric systems are addressed at the new and upcoming high-resolution RIXS facilities.

ACKNOWLEDGMENTS

This work was performed at the ADRESS beamline of the Swiss Light Source at the Paul Scherrer Institut, Switzerland and the entire staff is gratefully acknowledged. J.-E.R. gratefully acknowledges support by the Swedish Research Council (VR) under Grants No. 2014-04518 and No. 2018-04088. A.F. acknowledges funding by the ERC–Advanced Investigator Grant No. 669531 EDAX.

[1] P. Glans, P. Skytt, K. Gunnelin, J.-H. Guo, and J. Nordgren, Selectively excited X-ray emission spectra of N_2, J. Electron Spectrosc. Relat. Phenom. **82**, 193 (1996).

[2] M. S. Schöffler, J. Titze, N. Petridis, T. Jahnke, K. Cole, L. P. H. Schmidt, A. Czasch, D. Akoury, O. Jagutzki, J. B. Williams, N. A. Cherepkov, S. K. Semenov, C. W. McCurdy, T. N. Rescigno, C. L. Cocke, T. Osipov, S. Lee, M. H. Prior, A. Belkacem, A. L. Landers, H. Schmidt-Böcking, T. Weber, and R. Dörner, Ultrafast probing of core hole localization in N_2, Science **320**, 920 (2008).

[3] J. Nordgren, L. Selander, L. Pettersson, C. Nordling, K. Siegbahn, and H. Ågren, Core state vibrational excitations and symmetry breaking in the CK and OK emission spectra of CO_2, J. Chem. Phys. **76**, 3928 (1982).

[4] W. Domcke and L. Cederbaum, Vibronic coupling and symmetry breaking in core electron ionization, Chem. Phys. **25**, 189 (1977).

[5] P. Skytt, P. Glans, J.-H. Guo, K. Gunnelin, C. Såthe, J. Nordgren, F. K. Gel'mukhanov, A. Cesar, and H. Ågren, Quenching of Symmetry Breaking in Resonant Inelastic X-Ray Scattering by Detuned Excitation, Phys. Rev. Lett. **77**, 5035 (1996).

[6] F. Gel'mukhanov and H. Ågren, Resonant x-ray raman scattering, Phys. Rep. **312**, 87 (1999).

[7] F. Hennies, S. Polyutov, I. Minkov, A. Pietzsch, M. Nagasono, H. Ågren, L. Triguero, M.-N. Piancastelli, W. Wurth, F. Gel'mukhanov, and A. Föhlisch, Dynamic interpretation of resonant x-ray raman scattering: Ethylene and benzene, Phys. Rev. A **76**, 032505 (2007).

[8] S. A. Malinovskaya and L. S. Cederbaum, The role of coherence and time in the mechanism of dynamical symmetry breaking and localization, Int. J. Quantum Chem. **80**, 950 (2000).

[9] M. G. Vergniory, L. Elcoro, C. Felser, N. Regnault, B. A. Bernevig, and Z. Wang, A complete catalogue of high-quality topological materials, Nature **566**, 480 (2019).

[10] Y. Ma, P. Skytt, N. Wassdahl, P. Glans, J. Guo, and J. Nordgren, Core Excitons and Vibronic Coupling in Diamond and Graphite, Phys. Rev. Lett. **71**, 3725 (1993).

[11] S. Tanaka and Y. Kayanuma, Dynamics in resonant x-ray emission of the core exciton state: Competition between electron itinerancy and lattice relaxation, Phys. Rev. B **71**, 024302 (2005).

[12] F. Hennies, A. Pietzsch, M. Berglund, A. Föhlisch, T. Schmitt, V. Strocov, H. O. Karlsson, J. Andersson, and J.-E. Rubensson, Resonant Inelastic Scattering Spectra of Free Molecules with Vibrational Resolution, Phys. Rev. Lett. **104**, 193002 (2010).

[13] J.-E. Rubensson, A. Pietzsch, and F. Hennies, Vibrationally resolved resonant inelastic soft X-ray scattering spectra of free molecules, J. Electron Spectrosc. Relat. Phenom. **185**, 294 (2012).

[14] S. Schreck, A. Pietzsch, B. Kennedy, C. Såthe, P. S. Miedema, S. Techert, V. N. Strocov, T. Schmitt, F. Hennies, J.-E. Rubensson, and A. Föhlisch, Ground state potential energy surfaces around selected atoms from resonant inelastic x-ray scattering, Sci. Rep. **6**, 20054 (2016).

[15] S. Moser, S. Fatale, P. Krüger, H. Berger, P. Bugnon, A. Magrez, H. Niwa, J. Miyawaki, Y. Harada, and M. Grioni, Electron-Phonon Coupling in the Bulk of Anatase TiO_2 Measured by Resonant Inelastic X-Ray Spectroscopy, Phys. Rev. Lett. **115**, 096404 (2015).

[16] L. Braicovich, M. Rossi, R. Fumagalli, Y. Peng, Y. Wang, R. Arpaia, D. Betto, G. M. D. Luca, D. D. Castro, K. Kummer, M. M. Sala, M. Pagetti, G. Balestrino, N. B. Brookes, M. Salluzzo, S. Johnston, J. van den Brink, and G. Ghiringhelli, Determining the electron-phonon coupling in superconducting cuprates by resonant inelastic x-ray scattering: Methods and results on $Nd_{1+x}Ba_{2-x}Cu_3O_{7-\delta}$, arXiv:1906.01270v1.

[17] T. Schmitt, F. M. F. de Groot, and J.-E. Rubensson, Prospects of high-resolution resonant X-ray inelastic scattering studies on solid materials, liquids and gases at diffraction-limited storage rings, J. Synchrotron Radiat. **21**, 1065 (2014).

[18] A. Cesar, F. Gel'mukhanov, Y. Luo, H. Ågren, P. Skytt, P. Glans, J. Guo, K. Gunnelin, and J. Nordgren, Resonant x-ray scattering beyond the Born–Oppenheimer approximation: Symmetry breaking in the oxygen resonant x-ray emission spectrum of carbon dioxide, J. Chem. Phys. **106**, 3439 (1997).

[19] D. Maganas, P. Kristiansen, L.-C. Duda, A. Knop-Gericke, S. DeBeer, R. Schlögl, and F. Neese, Combined experimental and ab initio multireference configuration interaction study of the resonant inelastic x-ray scattering spectrum of CO_2, J. Phys. Chem. C **118**, 20163 (2014).

[20] P. J. Knowles, P. Rosmus, and H.-J. Werner, On the assignment of the electronically excited singlet states in linear CO_2, Chem. Phys. Lett. **146**, 230 (1988).

[21] J.-E. Rubensson, J. Söderström, C. Binggeli, J. Gråsjö, J. Andersson, C. Såthe, F. Hennies, V. Bisogni, Y. Huang, P. Olalde, T. Schmitt, V. N. Strocov, A. Föhlisch, B. Kennedy, and

A. Pietzsch, Rydberg-Resolved Resonant Inelastic Soft X-Ray Scattering: Dynamics at Core Ionization Thresholds, Phys. Rev. Lett. **114**, 133001 (2015).

[22] V. N. Strocov, T. Schmitt, U. Flechsig, T. Schmidt, A. Imhof, Q. Chen, J. Raabe, R. Betemps, D. Zimoch, J. Krempasky, X. Wang, M. Grioni, A. Piazzalunga, and L. Patthey, High-resolution soft X-ray beamline ADRESS at the Swiss Light Source for resonant inelastic X-ray scattering and angle-resolved photoelectron spectroscopies, J. Synchrotron Radiat. **17**, 631 (2010).

[23] G. Ghiringhelli, A. Piazzalunga, C. Dallera, G. Trezzi, L. Braicovich, T. Schmitt, V. N. Strocov, R. Betemps, L. Patthey, X. Wang, and M. Grioni, Saxes, a high resolution spectrometer for resonant x-ray emission in the 400-1600 eV energy range, Rev. Sci. Instrum. **77**, 113108 (2006).

[24] K. Okada, H. Yoshida, Y. Senba, K. Kamimori, Y. Tamenori, H. Ohashi, K. Ueda, and T. Ibuki, Angle-resolved ion-yield measurements of CO_2 in the O1s to rydberg excitation region, Phys. Rev. A **66**, 032503 (2002).

[25] A. Kivimäki, J. Alvarez-Ruiz, T. J. Wasowicz, C. Callegari, M. de Simone, M. Alagia, R. Richter, and M. Coreno, O 1s excitation and ionization processes in the CO_2 molecule studied via detection of low-energy fluorescence emission, J. Phys. B: At., Mol. Opt. Phys. **44**, 165103 (2011).

[26] J. Adachi, N. Kosugi, and A. Yagishita, Symmetry-resolved soft x-ray absorption spectroscopy: Its application to simple molecules, J. Phys. B: At., Mol. Opt. Phys. **38**, R127 (2005).

[27] K. C. Prince, L. Avaldi, M. Coreno, R. Camilloni, and M. de Simone, Vibrational structure of core to Rydberg state excitations of carbon dioxide and dinitrogen oxide, J. Phys. B: At., Mol. Opt. Phys. **32**, 2551 (1999).

[28] H. Romanowski, R. B. Gerber, and M. A. Ratner, The anharmonic stretching-bending potential of CO_2 from inversion of spectroscopic data, J. Chem. Phys. **88**, 6757 (1988).

[29] J. Laksman, E. P. Månsson, C. Grunewald, A. Sankari, M. Gisselbrecht, D. Céolin, and S. L. Sorensen, Role of the renner-teller effect after core hole excitation in the dissociation dynamics of carbon dioxide dication, J. Chem. Phys. **136**, 104303 (2012).

[30] F. Gel'mukhanov, P. Sałek, T. Privalov, and H. Ågren, Duration of x-ray raman scattering, Phys. Rev. A **59**, 380 (1999).

[31] A. Kivimäki, B. Kempgens, K. Maier, H. M. Köppe, M. N. Piancastelli, M. Neeb, and A. M. Bradshaw, Vibrationally Resolved O 1*s* Photoelectron Spectrum of CO_2: Vibronic Coupling and Dynamic Core-Hole Localization, Phys. Rev. Lett. **79**, 998 (1997).

[32] J. Söderström, M. Agåker, R. Richter, M. Alagia, S. Stranges, and J.-E. Rubensson, Oxygen K-edge x-ray-emission-threshold-electron coincidence spectrum of CO_2, Phys. Rev. A **76**, 022505 (2007).

[33] B. Zhou, C. Zhu, Z. Wen, Z. Jiang, J. Yu, Y.-P. Lee, and S. H. Lin, Topology of conical/surface intersections among five low-lying electronic states of CO_2: Multireference configuration interaction calculations, J. Chem. Phys. **139**, 154302 (2013).

[34] R. Feifel, A. Baev, F. Gel'mukhanov, H. Ågren, M. N. Piancastelli, M. Andersson, G. Öhrwall, C. Miron, M. Meyer, S. L. Sorensen, A. Naves de Brito, O. Björneholm, L. Karlsson, and S. Svensson, Generalization of the duration-time concept for interpreting high-resolution resonant photoemission spectra, Phys. Rev. A **69**, 022707 (2004).

[35] A. Spielfiedel, N. Feautrier, G. Chambaud, P. Rosmus, and H. Werner, The first dipole-allowed electronic transition $1\,^1\Sigma_u^+$ - X $^1\Sigma_g^+$ of CO_2, Chem. Phys. Lett. **216**, 162 (1993).

[36] R. McDiarmid and J. P. Doering, Electronic excited states of CO_2 : An electron impact investigation, J. Chem. Phys. **80**, 648 (1984).

[37] J.-E. Rubensson, RIXS dynamics for beginners, J. Electron Spectrosc. Relat. Phenom. **110**, 135 (2000).

[38] H. Veenhuizen, B. Wannberg, L. Mattsson, K.-E. Norell, C. Nohre, L. Karlsson, and K. Siegbahn, High resolution angle-resolved photoelectron spectrum of CO_2, excited with polarized resonance radiation, J. Electron Spectrosc. Relat. Phenom. **41**, 205 (1986).

[39] P. Baltzer, F. T. Chau, J. H. D. Eland, L. Karlsson, M. Lundqvist, J. Rostas, K. Y. Tam, H. Veenhuizen, and B. Wannberg, A study of the vibronic structure in the He I excited photoelectron spectrum of CO_2 involving the X $2\Pi_g$ and a $2\Pi_u$ ionic states, J. Chem. Phys. **104**, 8922 (1996).

[40] K. Gunnelin, P. Glans, P. Skytt, J.-H. Guo, J. Nordgren, and H. Ågren, Assigning x-ray absorption spectra by means of soft-x-ray emission spectroscopy, Phys. Rev. A **57**, 864 (1998).

[41] F. Kaspar, W. Domcke, and L. Cederbaum, The influence of finite lifetime of electronic states on the vibrational structure of molecular electronic spectra, Chem. Phys. **44**, 33 (1979).

[42] S. Cvejanovic and J. Jureta, Threshold spectrum of CO_2, J. Phys. B **18**, 2541 (1985).

[43] M. J. Hubin-Franskin, J. Delwiche, B. Leclerc, and D. Roy, Electronic excitation of carbon dioxide in the 10.5-18 eV range studied by inelastic electron scattering spectroscopy, J. Phys. B: At., Mol. Opt. Phys. **21**, 3211 (1988).

[44] F. Bloch and P. A. Ross, Radiative auger effect, Phys. Rev. **47**, 884 (1935).

[45] T. Åberg and J. Utriainen, Evidence for a "Radiative Auger Effect" in X-Ray Photon Emission, Phys. Rev. Lett. **22**, 1346 (1969).

[46] G. B. Armen, Spectator excitation accompanying radiative decay in atoms: A quantum defect model, J. Phys. B: At., Mol. Opt. Phys. **24**, 2467 (1991).